Parasitic heat load reduction of cryocoolers

E W Stautner[1], V Soni[1], A Wu[1], J Ricci[1]

[1]GE HealthCare – Technology & Innovation Center, Niskayuna, NY, 12309, USA

Email: ErnstWolfgang.Stautner@gehealthcare.com

Abstract. With the further advance of cryogenic technology and high helium cost, more cryogenic environments are designed to be hermetically "sealed", requiring a detailed understanding and analysis of parasitic heat fluxes crossing into a cryogenic environment. A thermal balance sheet therefore includes operational states but also needs to cover outages.

One of the frequently underestimated heat sources crossing the cryogenic boundary is a non-operating cryocooler attached to a cold mass. Once a cryocooler turns into a non-operating state, the cryocooler housing consisting of several stainless-steel tubes with internally stacked regenerator material creates a small, but steady parasitic heat conduction path to the cold mass.

Inclined, non-operating cryocoolers, however, follow the theory of inclined cryogenic tubes and operating inclined pulse tube coolers, delivering an excess heat flux to the cold mass that by a far exceeds any conductive thermal loads.

In this research paper we exemplarily determine the dominating parasitic convective heat flux created by non-operating GM cryocoolers. Moreover, we propose a simple process for shutting down this convective flow that is applicable for all types of non-operating cryocoolers, based on experimental results.

Keywords: Cryocooler, non-operating cryocooler, inclined cryocooler, vertical cryocooler, convective flow, thermal load reduction, thermal loss**.**

1. Introduction

Cryocoolers [1], [2], [3] are the workhorses in any commercial or research cryogenic environment with a well-established performance and reliability record over the last 50 years. One should therefore assume that these cryocoolers are well-characterized. However, as we make great strides to even further reduce the liquid helium inventory from over 1500 liters to barely 5 to 10 in so-called "sealed" MRI magnet systems little is known on what happens to this cryogenic environment if we shut down a cryocooler or suddenly lose power. Since the so-called allowed ridethrough time - the time until systems are powered up again (cooler downtime) -, is much shortened (less tolerable) with low helium inventory or purely conduction-cooled systems, we need to execute a more detailed cryogenic loss analysis that includes cryocoolers. During a ridethrough event all components warm up without one being able to control this warmup. When we calculate the losses that accelerate the warmup, the static heat losses for all components simply do not sum up as shown in Table 1. To some extent we can reduce those losses by addressing the magnet weight, suspension optimization and by ensuring thermal radiation is minimized. Still, there is one loss that has not been considered which becomes important during a cryostat and magnet warmup, and this is the cryocooler itself when shut down. Unfortunately, we do not have results from any cryocooler manufacturer detailing conduction and radiation losses. This paper reveals the loss effect of a shut-down cryocooler on the cryogenic environment, regardless of whether that is related to

IOP Conf. Series: Materials Science and Engineering **1344** (2026) 012103 doi:10.1088/1757-899X/1344/1/012103

a single or a multi-cooler system, although the event is even more critical with a single cooler. Multicoolers are sometimes used with one at standby or shut down and used for the purpose when excess operating cooling power is required, for example during a magnet ramp. In the following we look at single or multiple cryocoolers with one or several on standby and their failure mode and both, Gifford-McMahon (GM) and thermoacoustic based coolers (PTR) at low and high frequency operation. The following applies to a cryocooler installed on any cryogenic system.

Below examples are given for various cryocooler installs. As for MRI, coolers are mainly installed vertically whereas those by GE HealthCare are installed with 20 to 30 degrees inclinations.

Multiple cryocooler installation:

Known multicooler designs and cooler orientations, to name a few for example are:

- Superconducting (SC) generator GE [4] / EcoSwing [5] / SupraPower [6]
- GE HealthCare Compact 7 T (C7T) MRI system (inclined) [7], [8], [9]
- 7 T Siemens Magnetom Terra (vertical) [10] / GE HealthCare systems (vertical) [11]
- Rotating cryocooler on SC motor (horizontal) [12], [13]
- SC accelerators (vertical) and large detector magnets – (horizontal) [14]
- SC minesweepers etc. – (horizontal) [14]
- SC crystal pullers etc. – (vertical) [14]

GM type cryocoolers can be installed with an inclination angle or vertical whereas most low frequency PTRs are preferably installed vertical or only slightly inclined to minimize their performance loss.

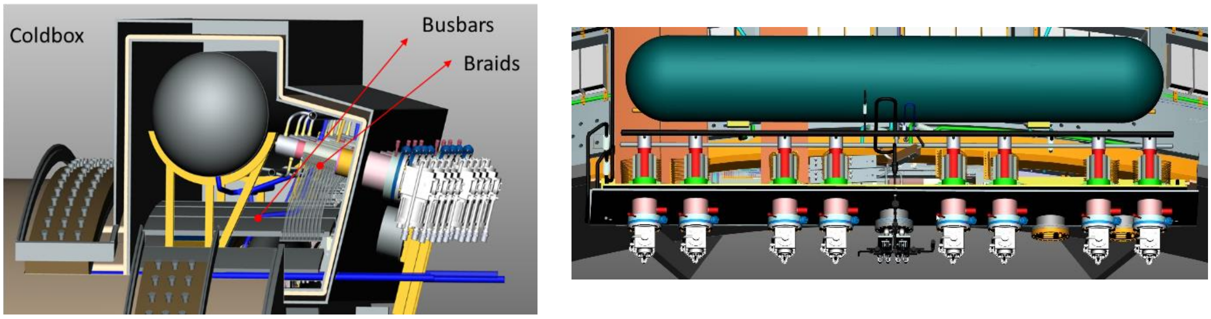

Figure 1. Superconducting 20 MW generator design
(a) Cryocooler location, (b) System architecture [4].

Figure 1 shows a superconducting magnet design with 6 Sumitomo SHI 412RDK cryocoolers (20-degree inclination) for steady state operational mode, with 2 additional ones on standby or idling and for coping with thermal transients as well as for maintenance. Below Figure 2 shows the new GE HealthCare HTIC MRI Compact 7 T (C7T) low cryogen magnet with 3 inclined (20 degree). A horizontally rotating cryocooler is shown in Figure 3 [12].

Rotating cryocooler installation, see for example [5], [6] and [12], [13]

Single cryocooler installation, see C3T MRI magnet (horizontal) [15]

Figure 2. GE HealthCare Compact 7 T System architecture with SHI RDK412 cryocooler arrangement (a) and field recording (b) [7], [8], [9].

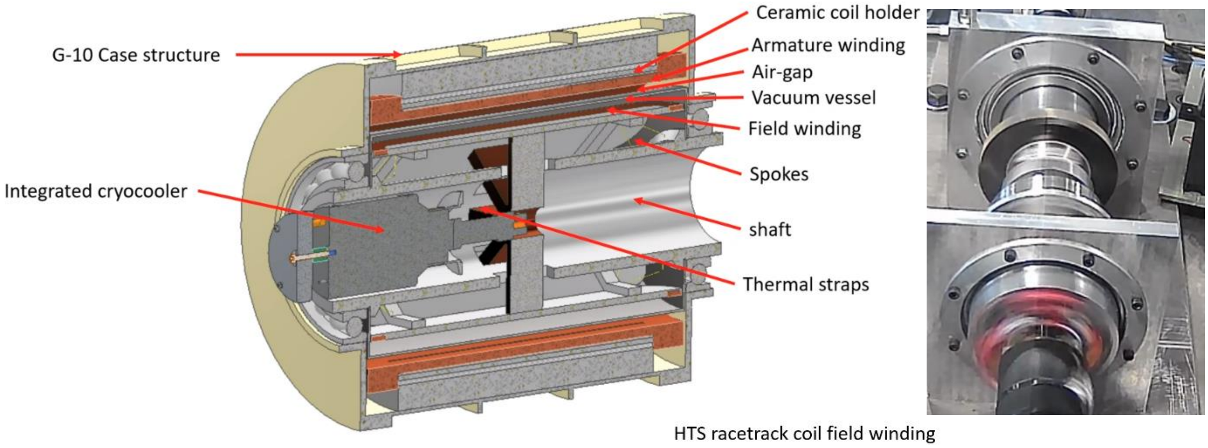

Figure 3. Horizontal mounting of a Stirling type cryocooler on a SC motor (left), rotating (right) [12].

2. Key development steps of GM coolers

GM cryocoolers consist of a motor housing with a rotary valve connected to a first and second stage regenerator piston sealed against the cryocooler sleeve housing. Early designs allowed for a higher leakage flow shown in Figure 4 (top), acting against the main flow with somewhat reducing cryocooler power at the stages, when installed inclined [14]. In 2015 [16] the design was improved to minimize this leakage flow using a spiral seal (Figure 4 bottom) that resulted in much-reduced inclination sensitivity shown on the right in Figure 4.

As mentioned, the angular influence is highly dependent on the cooler operating frequency. However, this effect is very small for cryocoolers such as Stirling type pulse tube coolers, operating at high frequencies in the 50 Hz range.

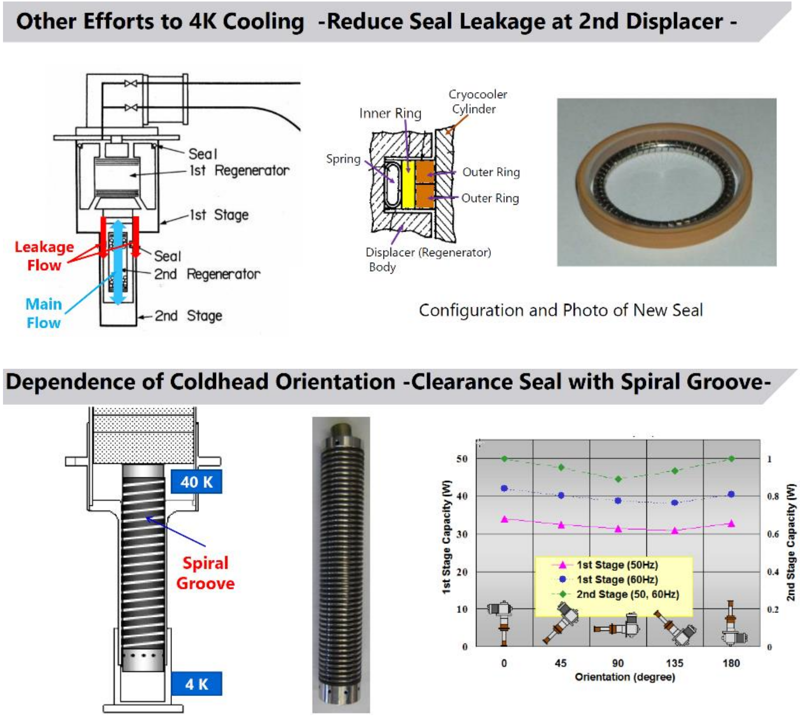

Figure 4. Leakage flow and angle influence for GM coolers vs PTRs [14].

3. Analysis

Once a design decision has been made for shutting down a cryocooler one needs to estimate how much heat would be transferred to the cryogenic environment as shown in the example in Figure 2 for a typical GM cooler second stage. For that we need to agree on some assumptions, for example we keep the 1st stage temperature relatively constant which normally is the case for some multi-cooler arrangements, but the thermal shield and the cold mass will drift up to higher temperatures for single cryocooler installs, as shown in Table 1.

Breakdown of thermal pathways and losses for a stopped, gaseous helium filled cryocooler.

What happens if we switch off a cryocooler, stopping the piston gas flow movement and heat exchange in the regenerator matrix, shuttle losses etc.? Cryocooler pistons run with a small clearance space (expansion chamber) on the cryocooler sleeve tube bottom. The cryocooler piston does not hit the bottom of the cryocooler housing nor does the 4 K stage stops at the housing bottom when shut down. The thermal path consists of the outer stainless-steel tube shell (housing) of the cryocooler with the thermally shortened bottom path due to the required copper heat transfer area. Typically, the upper housing diameter is approx. > 85 mm with the bottom shell (housing) varying between 40 to 43 mm, depending on cooler type. The cylindrical shell houses the displacer running at a typical stroke of 25 mm.

As Xu [17] noted during a stoppage there is a pulse tube cooling effect in the clearance space between cylinder and displacer. Figure 5 shows the known thermal pathways at the second stage [14] with calculated losses given in Table 1.

IOP Conf. Series: Materials Science and Engineering **1344** (2026) 012103 doi:10.1088/1757-899X/1344/1/012103

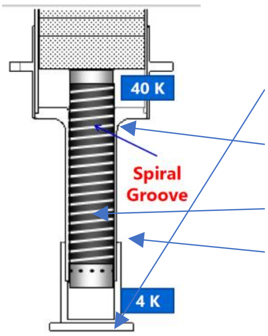

Figure 5. Cryocooler thermal path breakdown (2^{nd} stage) [14].

Table 1. Typical loss table averaged for GM cooler at shutdown

Loss type	**1^{st} stage**	**2^{nd} stage**	**Comment**
Shuttle heat transfer losses	0	0	Displacer stopped (not zero for idling coolers operating at very low frequency to compensate for losses)
Thermal radiation losses	5.7	0	[17]
Axial thermal conduction (wall)	5.4	0.33 [17]	0.28@ 45 K; 0.55 W @ 65K; 0.914 W @ 95K
Pulse tube effect	0	0.02 [17]	Spiral groove clearance, non-operating mode
Spiral groove contact	Tbd.	Tbd.	Losses to tube housing, contact resistance
Static helium conduction losses	1	0	Helium stratification assumed

Since the above static losses cannot explain the warmup speed, another overlooked parasitic loss mechanism, not covered yet, may be responsible.

4. Parasitic losses due to "secondary flow"

We presume that convective flow currents are started due to temperature differences within the cooler. Those parasitic flow caused thermal losses are well-known to reduce the cooling power of pulse tube cryocoolers and to a certain degree with an older GM cryocoolers without the implemented spiral seal [17] that is now stopping the convective flow between tube wall and gas. Since the cooler is not running, we need to consider a typical constant equalization pressure (EP) for the cooler at 1.5 to 1.6 MPa. Figure 6 schematically depicts the flow regimes developing within pressurized helium tubes. The arrows indicate the parasitic flow regime in vertical as well as inclined helium filled tubes or annular gaps with cryocoolers. Figure 6 (a) shows the PTR modeled as a helium filled tube and the GM cooler (b), (c) respectively, with an annular flow passage in the presence of a stationary piston.

Losses are different between GM and PTR coolers. We can distinguish between:

- Parasitic heat flux in a GM cryocooler with helium at equalization pressure
- Parasitic heat flux in a PTR with helium at equalization pressure
- Heat flux in vertical cryocooler orientation
- Heat flux in inclined cryocooler orientation

Simulating flow patterns and losses of a helium gas filled tube - whether vertical or inclined - is a difficult and time-consuming task with the need for multiple CFD runs. Groundbreaking research work has been done by Langebach [18] projecting the behavior of inclined tubes based on mapping the CFD analysis to an EES tool [19] shown in Figure 7. By adhering to the projected CFD boundary conditions this can give us a first estimate of the parasitic flow at each angle configured within a cooler.

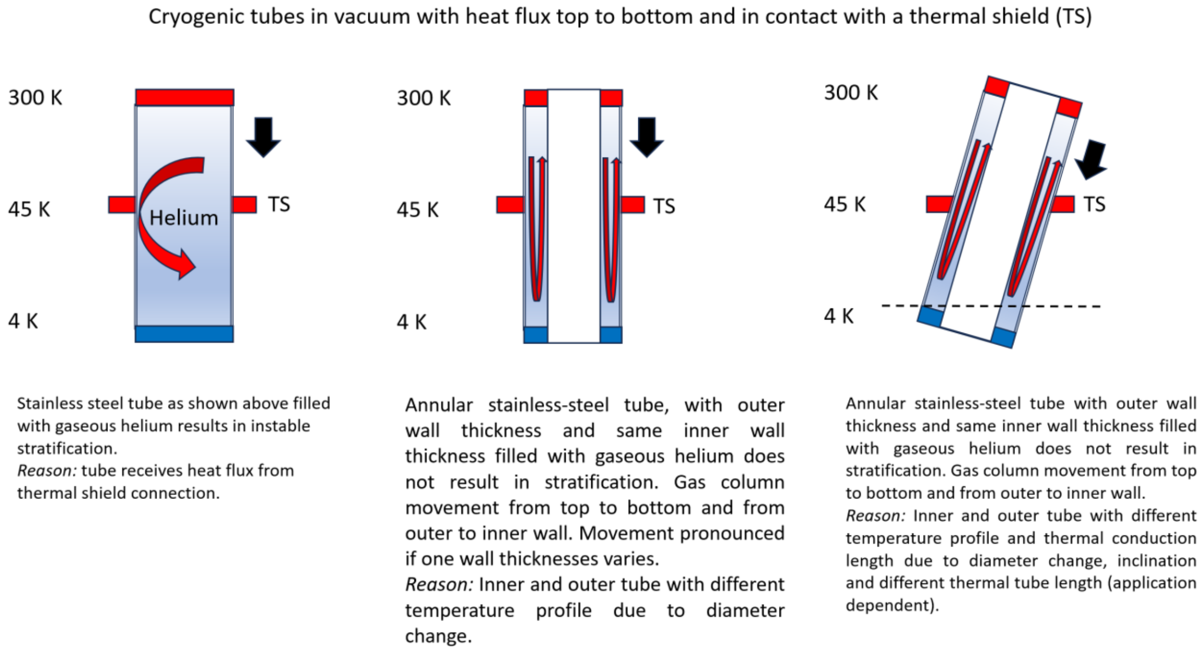

Figure 6. Inclination influence of closed helium filled tubes (a) and GM / PTR (b), (c) tube annulus.

5. Simulation effort and estimate

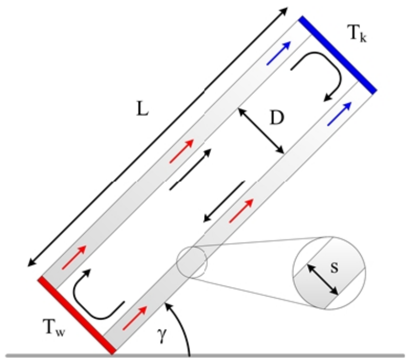

T_w = 270 [K] D = 0.006 [m]
T_k = 7 [K] L = 0.405 [m]
λ_{wall} = 3 [W/m-K] s = 0.0015 [m]
p = 15 [bar]

Raleigh number
Ra_D: = 4.86 10^5
Pipe closed at both ends (rotary valve closed)
Medium: Helium

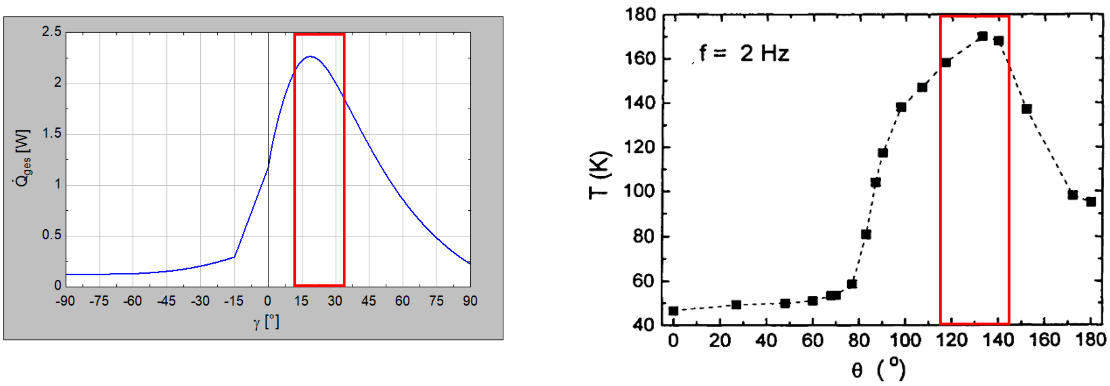

γ = - 90° = cold end down θ = 0° = cold end down
γ = +90° = cold end up θ = 180° = cold end up

a) b)

Figure 7. a) Simplified CFD extrapolations within valid boundaries for cryocooler gravity effect [18], [19] b) Pulse tube cooler orientation effect [20], [21]. Simulation does not include thermal radiation.

We find that parasitic convection currents increase with higher gas pressure in the tube, bigger tube wall thickness, increased inner tube diameter and higher tube wall thermal conductivity. They decrease with increasing tube length and higher cold end temperature. The above calculation is based on several cooler geometry related assumptions leaning on Xu [17]. For the convective parasitic flow calculation, we use the clearance space (annulus) between cylinder and displacer. Since the convective flow is from room temperature down to 4 K omitting any thermal shield coupling, we assume an annular clearance area at the 1^{st} and 2^{nd} stage and take the average of this up to room temperature. From that area we then calculate the “open” diameter for the convective flow which is around 6 mm for a total cooler heat transfer length of 0.4 m. The equalization pressure when the cooler has stopped is taken as 1.5 MPa. We assume a tube wall thickness of 1 to 2 mm, where 0 means horizontal operation, -90^{o} with the cold end at the bottom and 90^{o} cold end at the top. The cooler is installed at an angle of 20^{o}. Since the cold end immediately warms up to > 4 K a partly stationary temperature of 7 K is assumed. Any contact to a thermal shield that rises the 1^{st} stage temperature of the cooler is disregarded. This is mostly acceptable for a range of coolers where only one cooler is shut down. On the right we see a coaxial PTR with temperature vs inclination at a frequency of 2 Hz [20], [21] and on the left a simulated convective circulating heat flow in a shut cryocooler vs inclination angle showing a striking similarity. This also applies for systems with remote drives on PTRs. Ballpark Figure 7 results will be checked against time consuming CFD calculations and verified experimentally.

5.1. Experimental verification and impact of internal cryocooler structure on heat burden

Since we now have a better understanding on the loss magnitude and understanding the heat transfer mechanism from the warm to the cryocooler cold end vertical or inclined, we can stop the gas/wall heat transfer by simply removing the heat exchange medium (helium gas) to reduce the conduction heat burden on the magnet cold mass when the cryocooler is in an OFF state. For the test the 20 degree operating angle (for service reasons) of the GE HealthCare cryocooler according to the theory described above hits the point where the parasitic heat load is at its maximum. The results confirm the following: although the cryocooler piston cartridges (see Figure 5) are filled with spheres and steel meshes it is clear from the experiments that a parasitic heat load indeed occurs mainly in the annulus clearance space rather than through the regenerator housing piston and therefore behaves like a tube as shown in Figure 6 b/c. Furthermore, the cryocooler behaves like an inclined tube with flexlines disconnected, (closed warm end) as shown in the introduction of this paper. For a more in-depth review and understanding of the effect of inclined tubes, see Chapter 6 of “Aircraft cryogenics”, [22].

Pump attached to cryocooler motor (shown with open motor shielding), 20-degree inclination, with cryocooler flexlines removed

Figure 8. C7T MRI magnet and cryocooler assembly with attached vacuum pump [9].

An exemplary automatic control schematics with piping to compressor and pump lines for removing helium from a cryocooler attached to a cold mass is given in [23].

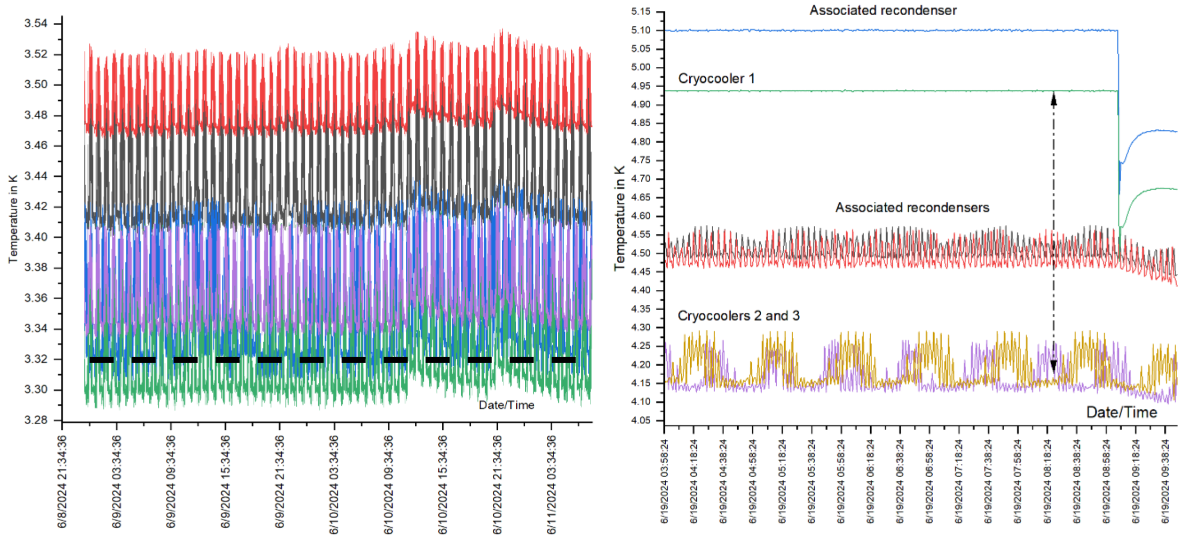

Figure 9. a) Initial state of the cryocoolers (dotted line average) b) After shutting down cooler 1.

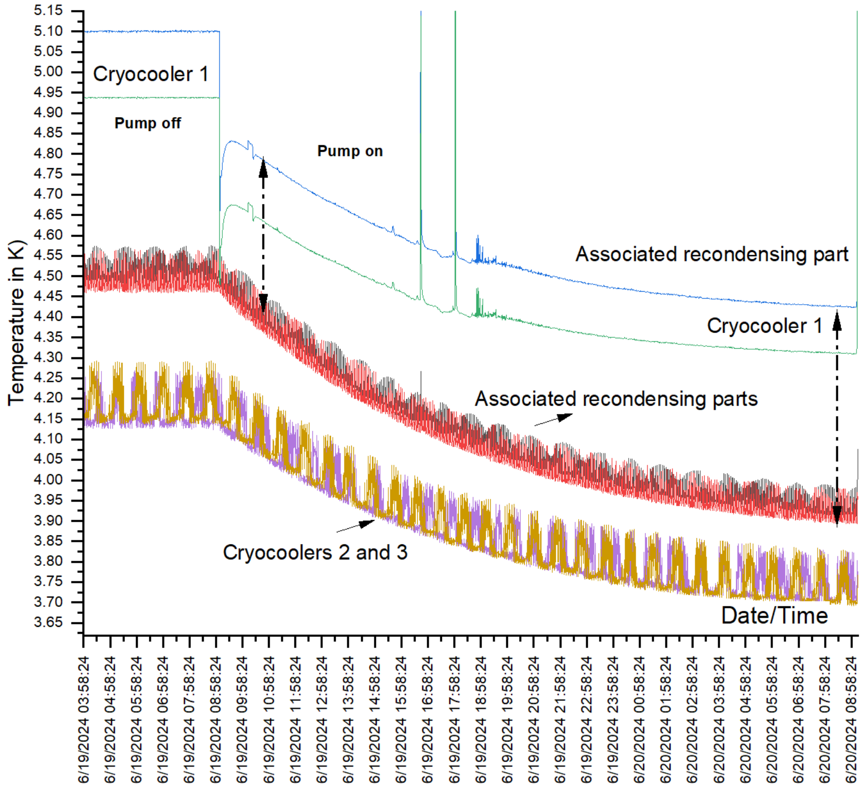

Figure 10. C7T MRI magnet single cryocooler pump-out temperature recovery (Figures 2 and 8).

IOP Conf. Series: Materials Science and Engineering **1344** (2026) 012103 doi:10.1088/1757-899X/1344/1/012103

Figure 9 a) shows the temperatures of the 3 recondensers and the 3 cryocoolers in operation. Note the dotted line shows the average temperature of the 3 cryocoolers whereas the other curves shows the dT of the individual 3 attached recondensers. Figure 9 b) shows the state where cryocooler 1 is switched off together with the attached recondenser showing as true straight line indicating no piston movement. Note that the temperature baselines has changed significantly from 3.32 K to 4.2 K with cryocooler 1 recondenser now no longer recondensingat 5.1 K. Figure 10 depicts the two states in more detail with, Cooler 1 at shutdown and after evacuation. The horizontal line on the left shows the temperature of the cold end of Cooler 1 with attached recondensing part (above line) when shut down as in Figure 9 b, without showing the characteristic oscillating wave form caused by the piston cycle seen when cryocoolers are running (2, 3). Cooler 1 can no longer recondense causing a cold mass base line shift from 3.32 to 4.2 K when all 3 coolers are running. When Cooler 1 is turned off the parasitic heat load on the attached condenser cup creates a pressure gradient in the connecting lines to coolers 2 and 3 causing a temperature rise, now assuming the new, averaged baseline temperature of 4.2 K. We then evacuated Cooler 1 (pump on state) thereby eliminating the main parasitic heat flux as discussed in Figure 7. With reduced heat burden, the pressure gradient in the lines reduces and Cooler 1 starts to cool down again. Not only is Cooler 1 now 0.5 K colder than before evacuation, but the cooling effect also propagates through both running coolers 2 and 3 resulting in a heat burden shift from an average of 4.2 K (pump off) to less than 3.7 K (pump on) (stopped before reaching equilibrium) close to the 3.5 K base temperature when all 3 coolers are in operation. Consequently, more helium can now be recondensed. Returning to a lower base temperature is key for increasing the mentioned ridethrough time especially on low cryogen or conduction-cooled systems, e.g. for gaining extended cryocooler service time for the field engineer to arrive on site, or from benefitting from a larger time window for any magnet field rundown or other. In this configuration we thermally neutralized the shut-down cryocooler from the cryogenic environment by evacuating the cooler and removed approx. 1.35 W from the cryogenic circuit, not too far off from an estimated theoretical heat loss for inclined tubes with a 20-degree convective/conductive loss maximum.

A word of caution on shut down pulse tube coolers installed vertically. For most PTRs it is unlikely that they would initiate thermoacoustic oscillations on a 4 K tube, nevertheless the parasitic load on some shutdown PTRs due to intrinsic gas movement and tube conductance can still be substantial and should not be disregarded.

6. Summary

By reducing cryogenic cold mass weight and size of the cryogenic envelope we addressed the reduction of thermal conduction and radiation losses for low cryogen, compact sealed MRI magnet systems. We now found that cryocooler shutdown severely increases the total cryogenic loss balance reducing ridethrough times due to its intrinsic parasitic losses. Shut down cryocoolers show cryogenic thermal regimes related to inclined tubes. Cryocooler evacuation with disconnected compressor flexlines is seen as an efficient means to substantially increase ridethrough. It is suggested to install features that automatically remove helium in the event of a cooler shutdown to eliminate convection currents as the major parasitic heat source. A detailed CFD analysis will provide further insight into the cryogenic flow patterns of inclined idling or shutdown cryocoolers.

Acknowledgement
for NIH contract award NIH U01EB027696

References

[1] Walker G Cryocoolers Part 1 and 2 The International Cryogenics Monograph Series Plenum Press 1983
[2] Stautner W Cryocoolers for Superconducting Generators Chapter 6 in Atrey M (ed.) Cryocoolers – Theory and Applications International Cryogenics Monograph Series Springer Publishing 2020

IOP Conf. Series: Materials Science and Engineering **1344** (2026) 012103 doi:10.1088/1757-899X/1344/1/012103

[3] Stautner W Cryocoolers for Healthcare Chapter 9 in Atrey M (ed.) Cryocoolers – Theory and Applications International Cryogenics Monograph Series Springer Publishing 2020
[4] Stautner W Torrey D Xu M Wu A Parizh M Soni V Cryogenic aspects of a 20 MW class low-temperature superconducting generator for the renewables industry 2024 *IOP Conf. Ser.: Mater. Sci. Eng.* **1301** 012048
[5] Bergen et al Design and in-field testing of the world's first ReBCO rotor for a 3.6 MW wind generator Supercond. Sci. Technol. 32 (2019) 125006
[6] Bilbao I M SUPRAPOWER: Superconducting, reliable, lightweight, and more powerful offshore wind turbine Final report 2017
[7] Wu A Ricci J Conte G van Epps C Xu M Bai Y Parizh M Stautner W Hua Y Vermilyea M Soni V Foo T Design and Construction of a Low-Cryogen, Lightweight, Head-Only 7 T MRI Magnet in *IEEE Transactions on Applied Superconductivity* vol 34 no 5 pp 1-5 2024 doi:10.1109/TASC.2024.3352551
[8] Foo T et al Compact 7T: Progress in construction and assembly of a low-cryogen, high-performance, head-only high-field MRI system in Proc. 31st Sci. Meeting ISMRM 2023
[9] Soni V Stautner W C2Po3A-08 Cryogenic Cooldown Performance of the GE (HTIC) Compact 7 T MRI Magnet CEC/ICMC Reno NV 2025
[10] Siemens 7 T magnet Terra https://www.siemens-healthineers.com/en-us/magnetic-resonance-imaging/7t-mri-scanner/magnetom-terra?gad_source=1&gbraid=0AAAAAD_HlgtzXGQXIuhr1Du-0Jm-gvtCG&gclid=Cj0KCQjw2ZfABhDBARIsAHFTxGynCc8A54yB57GFBpclp_qS5x8CyNY0OL1TqqQ5kAtRLhErSo-ITmMaAnVWEALw_wcB
[11] GE 7 T Signa https://www.gehealthcare.com/products/magnetic-resonance-imaging/7t-mri-scanner
[12] Balachandran T Kovacs C Ansell P Stautner W Bong U Xiao J Sirimanna S Salk N Bauer Venkataraman R Haugan T Sumption M Haran K M2Or4A-04 Overview and Progress Update on a Superconducting Powertrain for CHEETA CEC/ICMC 25 Reno NV 2025
[13] Balachandran T Salk N J Xiao J Sirimanna S Bong U Zhao Y Haran K et al Advancements in Superconducting Electric Propulsion: Comparative Analysis and Progress Update of CHEETA and CRUISE Motors in *IEEE Transactions on Applied Superconductivity* vol 35 no 5 pp 1-5 2025 doi: 10.1109/TASC.2025.3538003
[14] Kuriyama T Development of a 4 K-GM cryocooler and its applications for superconducting magnets ICEC29/ICMC2024 Geneva 2024
[15] Foo T Laskaris E et al Lightweight, compact, and high-performance 3 T MR system for imaging the brain and extremities Magn Reson Med 2018 Nov 80(5):2232-2245 doi: 10.1002/mrm.27175. Epub 2018 Mar 13
[16] Ikeya Y Expanding market of a 4 K GM cryocooler International Congress of Refrigeration 24 Yokohama Japan 2015
[17] Xu M Y Morie T Numerical Simulation of a 4 K GM Cryocooler International Cryocooler Conference Inc. 17 Boulder CO 2012
[18] Langebach R Haberstroh C Natural convection in inclined pipes - A new correlation for heat transfer estimations AIP Conf. Proc. 1573 pp 1504–1511 2014 https://doi.org/10.1063/1.4860885 and private communication
[19] EES Engineering Equation Solver V11 http://fChartSoftware.com
[20] Thummes G Schreiber M Landgraf R Heiden C Convective Heat Losses in Pulse Tube Coolers: Effect of Pulse Tube Inclination Cryocoolers 9 Plenum Press NY 1997 pp 393-396
[21] Shiraishi M Murakami M Nakano A Iida T Visualization of Secondary Flow in an Inclined Double-Inlet Pulse Tube Refrigerator Cryocoolers 14 International Cryocooler Conference Boulder 2007
[22] Stautner W Aircraft Cryogenics International Cryogenics Monograph Series Springer 2024
[23] Stautner W Soni V Wu A 2025 patent pending